



## Post-Fire Ship Hull Repair Method Considering Corrosion Rate and Mechanical Properties

Imam Baihaqi<sup>1\*)</sup>, Heri Supomo<sup>1)</sup>

<sup>1)</sup>Department of Naval Architecture and Shipbuilding Engineering, Sepuluh Nopember Institute of Technology, Surabaya 60111, Indonesia

<sup>\*)</sup> Corresponding Author: [imam.baihaqi@its.ac.id](mailto:imam.baihaqi@its.ac.id)

### Article Info

### Abstract

#### Keywords:

Post-fire,  
ship hull repair,  
corrosion rate,  
3-cell electrode,  
repair method

#### Article history:

Received: 12/03/2025  
Last revised: 22/04/2025  
Accepted: 22/04/2025  
Available online: 25/04/2025  
Published: 25/04/2025

#### DOI:

<https://doi.org/10.14710/kapal.v22i1.71686>

Ship accidents due to fire result in several consequences, especially concerning the structure and strength of the ship. The very high temperature of the ship fire greatly affects the mechanical properties and corrosion resistance of the ship's construction materials after the fire exposed. This study investigated the relationship between corrosion resistance and mechanical properties of materials which were heat-treated due to fire. In this experimental study, the post-fire burnt plate was simulated by heating the new ship plate in a muffle furnace. The seawater medium directly cooled the heat-treated ship plates in each temperature's variation until they reached room temperature. The experimental temperature variations used are 300°C, 500°C, 600°C, 700°C, and 900°C. The corrosion resistance tests were carried out using the 3-electrode cell method. The study results show that the higher the temperature of the ship fire burnt, the corrosion speed increased significantly, reaching a peak at about 2.5 mmpy at 600°C. After achieving the maximum rate, the trend decreased until reaching a similar value as a non-heat-treated plate. When these corrosion rate results are associated with mechanical properties results (tensile tests based on the same heat treatment), the tensile strength of the material has a gradual increasing trend in higher heat-treated temperatures applied. It indicates that the hardness grade of the ship plate became higher due to the heat-treatment process. Based on both considerations results, the steel plate can still be re-used or refurbished if the temperature is below 600°C, with a tensile strength of 445 MPa and a corrosion rate of about less than 0.5 mmpy.

Copyright © 2025 KAPAL: Jurnal Ilmu Pengetahuan dan Teknologi Kelautan. This is an open access article under the CC BY-SA license (<https://creativecommons.org/licenses/by-sa/4.0/>).

## 1. Introduction

Shipwreck accidents occur frequently in Indonesia. According to data from the National Transportation Safety Committee (KNKT), 15 out of 36 investigated accidents between 2007 and 2016 were caused by fires or explosions, making them the most common cause of shipwrecks. These incidents were followed by sinking accidents, which accounted for 11 cases, and collisions, which made up of 10 cases. The KNKT report [1] also reveals the significant human suffering of these fire-related accidents, with 736 fatalities and 605 injuries recorded during this period. The latest data investigation report from KNKT presented that between 2020 and 2024, there were about 5–6 shipwreck accidents due to burning annually, which is quite frequent [2].

Fire incidents on ships lead to casualties and injuries and cause significant financial losses due to damage. Fires can significantly affect the cargo in transit, potentially resulting in its total destruction. Besides cargo damage, fires also affect the ship itself, causing harm to three main components: the ship's structural construction, the machinery systems, and the equipment systems. This extensive damage can result in substantial repair and replacement costs. After the fire, parts of the ship's structure may undergo partial deformation due to decreased steel strength when exposed to burning heat; others do not undergo distortion. Only heat-induced heat flash effects can expose other construction parts. To ensure the ship's structural integrity, it needs further investigation into the justification for reusing, repairing, or replacing the ship hull structure.

Understanding the post-fire mechanical properties of structural steels is crucial for evaluating the residual performance and safety of steel structures after fire exposure. A wide array of studies has investigated the effects of elevated temperatures, cooling methods, and steel types on mechanical degradation, with significant implications for structural assessment, repair, and design.

Wang and Liu [3] conducted an experimental study on Q690 high-strength steel, focusing on several influencing factors such as heating rate, cooling method (air vs. water), repeated heating cycles, and pre-applied loading. The study measured post-fire elastic modulus, yield strength, tensile strength, and fracture strain. They found that post-fire yield strength decreased significantly as the exposure temperature increased, especially when heated above 400°C with air cooling or 500°C with water quenching. However, tensile strength increased for specimens quenched after heating above 700°C due to

martensite formation. Similarly, Dan et al. [4] investigated four structural steel types (Q345, Q460, Q550, and Q690) through controlled fire exposures from 300°C to 800°C followed by air cooling. Their study introduced a comprehensive stress-strain model that incorporates the influence of fire temperature on elasticity, yield plateau, and plasticity. They confirmed that mechanical degradation begins beyond 600°C, and the residual factors followed predictable functions—either exponential or linear—depending on the steel grade.

For medium-grade steels, Shi et al. [5] examined the post-fire behavior of Q345 base metal and welds. Their coupon tests assessed stress-strain response, yield strength, and ductility after fire exposure up to 1000°C. The study developed predictive formulas for engineers and found that water cooling increased strength but reduced ductility, while air cooling maintained higher ductility but lower strength. Li and Young [6] focused on cold-formed high-strength steels with nominal strengths of 700 MPa and 900 MPa. Using tensile coupon tests, they measured stress-strain behavior after heating from 200°C to 1000°C. The study developed empirical equations for post-fire yield stress and ultimate strength, confirming that strength deteriorates gradually with increasing fire exposure.

Advanced cold-formed steels were explored by Yan et al. [7], who tested dual-phase and martensitic steels. Their results revealed that these steels experienced early, and more severe strength degradation compared to conventional cold-formed steels. They introduced retention factors and a predictive model to quantify strength loss, emphasizing that cold-formed advanced steels are more vulnerable in fire scenarios. Gordon et al. [8] added a unique dimension by analyzing the impact of heating duration on A572 Gr. 50 steel. By varying exposure time (0.5 vs. 2 hours) and temperature (500– 800°C), and using Vickers microhardness and microscopy, they showed that longer exposure time led to greater degradation at 700°C, but had less effect at 800°C, underscoring the importance of time in post-fire analysis.

In marine applications, Baihaqi et al. [9] and Komariyah et al. [10] provided crucial insights. Baihaqi et al. [9] investigated the fire exposure of low-carbon ship steel plate using furnace heating followed by seawater quenching. They observed increased tensile strength above 600°C but reduced ductility beyond 700°C, suggesting replating is viable only below certain thresholds. Komariyah et al. [10] used destructive testing and metallography on actual fire-exposed ship structures, noting softening in slow-cooled areas due to annealing and confirming the absence of martensitic embrittlement in water-sprayed zones. Overall, these studies highlight the complex interplay of temperature, steel type, cooling method, and duration in determining post-fire performance.

On the other hand, the degradation of marine structural steels due to fire exposure and prolonged corrosion in aggressive marine environments has been extensively studied. Shen [11] explored the performance of super-ferritic stainless steel (SFSS) under fire-like temperatures, finding that although SFSS exhibits high mechanical strength (~600 MPa) and low corrosion rates (0.03 mm/year) in chloride-rich environments, exposure to 700– 800°C reduces its ductility significantly and increases corrosion rates to 0.4 mm/year. This indicates a strong risk of post-fire corrosion even in corrosion-resistant materials. Ren et al. [12] analyzed the mechanical performance of D36 steel after corrosion and subsequent heating to 500°C and 900°C. Their findings showed significant tensile strength reduction and microstructural degradation, indicating that heat and corrosion synergistically reduce the mechanical integrity of marine steels. Similarly, Kumar et al. [13] reported that interstitial-free (IF) steel subjected to salt spray corrosion lost mechanical strength rapidly once mass loss exceeded 3%, emphasizing the critical impact of surface damage and pitting.

From a protection perspective, Abdel-Samad et al. (2014) highlighted the effectiveness of marine coatings, particularly “HEMPALIN ENAML 52140,” which demonstrated the lowest corrosion rate (0.8 mm/year) and up to 77% protection in salt spray tests. Garbatov and Guedes Soares [14] proposed a probabilistic model for predicting steel surface wastage using real-world corrosion data, offering a useful tool for life-cycle maintenance planning. Long-term field exposure studies further validate laboratory data. Vukelic et al. [15], [16] found that AH36 steel exposed for up to 36 months in splash zones developed deep pitting, mass loss, and reduced tensile and impact strength. Huang et al. [17] observed multi-layer rust formation and crack development on AISI 4135 steel in splash zones, which accelerated localized corrosion.

Material selection and microstructural design are key considerations. Gao et al. [18] showed martensitic steels with chromium enrichment resisted corrosion better than ferrite-pearlite steels in tropical marine exposure. Post-fire behavior, as shown by Zhang et al. [19] and Lee et al. [20], varies depending on the cooling method—rapid cooling improves strength but reduces ductility, while slow cooling maintains ductility. The literature shows that marine steels degrade significantly under combined effects of corrosion and fire exposure, especially in splash zones. Material microstructure, protective coatings, and environmental exposure history all influence performance. Therefore, selecting proper materials, applying durable coatings, and understanding post-fire behavior are essential for the long-term integrity of marine structures.

To the best of the authors' knowledge, there is very few research exploring the relationship between the mechanical properties of mild steel ship structures and their corrosion rates after fire exposure. Furthermore, the consideration of both results has not adequately addressed the implications for deciding whether to replace, repair, or reuse specific components. This article aims to investigate the findings from experimental tests and a literature review concerning the corrosion resistance and the mechanical properties of ship hull plate after being exposed to fire. Furthermore, it highlights their impact on methods for repairing ship hulls.

## 2. Methods

This study aims to investigate the effect of elevated burning temperatures on the corrosion rate of ship hull plates. The ship plates were cut into specific sizes about 200 mm x 300 mm which were heated in a muffle furnace with direct heating rate to specific temperatures of 300°C, 500°C, 600°C, 700°C, and 900°C. After reaching each target temperature (without any holding time), the heat-treated plates were rapidly cooled using seawater until achieving room temperature. The heat-treated plate were then cut into specific sizes before conducting corrosion test by using a three-electrode cell system. Before the tests, epoxy glue was used to separate certain areas of the specimens, leaving a 1 cm x 1 cm area that can be submerged in artificial-prepared seawater during the corrosion tests. The following sub-sections provide a more detailed explanation of the materials and methods.

## 2.1. Plate burning and cooling process

The first step in the experimental procedure involves heating the plate and then cooling it in a muffle furnace. The experiment used a new mild steel plate that is the same as ASTM A36 [21]. Its chemical composition is shown in Table 1, which is taken from the steel mill certificate. The elevated temperature variations applied during the heating process are listed in Table 2, ranging from 300 to 900 degrees Celsius. The ambient temperature is used as a benchmark for comparing the changes observed in the experimental results.

Table 1. Chemical composition of A36 carbon steel material plates (%)

C	Si	Mn	P	S	Al
0.173	0.130	0.983	0.018	0.005	0.046

Table 2. Burning elevated temperature variation of the steel plates.

Specimen Code	1	2	3	4	5	6
Temperature (°C)	Ambient	300	500	600	700	900

The steel plates were heated in a muffle furnace, as shown in Figure 1, according to the specified elevated temperature variations. Using a direct heating rate method, each target temperature was achieved. Without any holding time when achieving each target temperature, the steel plate was then rapidly cooled by seawater. The steel plates treated at different elevated temperatures are presented in Figure 2, which shows that higher temperatures result in the plates becoming progressively darker in color.



Figure 1. Simulation of burnt ship plates in Furnace

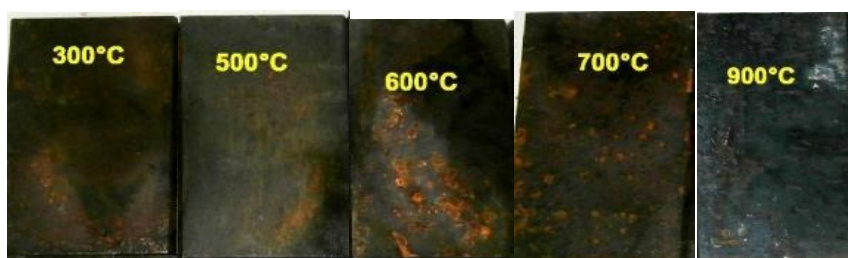


Figure 2. Ship plates that have been burnt from temperature of 300°C to 900°C, rapid-cooled by seawater

## 2.2. Specimen test for corrosion experiment

The specimens used for testing the corrosion rate of the steel plates have dimensions of 25 x 50 mm, in accordance with the standard reference test method for making potentiostatic and potentiodynamic anodic polarization measurements [22]. Each specimen was polished using sandpaper with a grit size of 120 to ensure a consistent surface roughness. After polishing, the specimens were coated with epoxy glue, leaving an exposed area of 1 cm<sup>2</sup> uncoated for testing (Figure 3). The top part of the specimen is also left uncoated to allow for attachment with crocodile clips, which are connected by cables to serve as the working electrode during the tests.

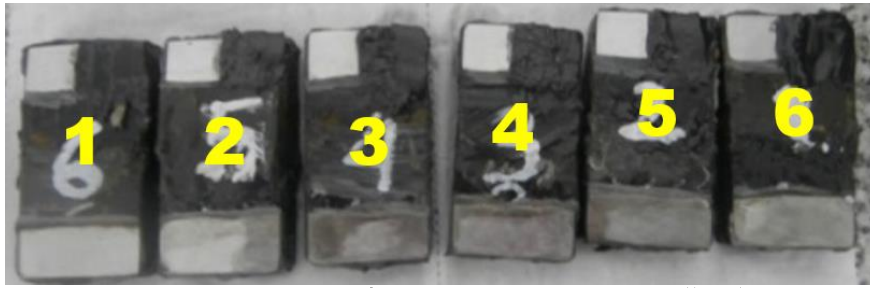


Figure 3. Prepared specimen for corrosion testing using cell 3 electrodes

### 2.3. Corrosion testing process

Once the specimens were ready for testing, the next step was to prepare the materials and equipment for the corrosion test. In this experiment, a 0.1 M NaCl electrolyte solution was prepared to conduct the corrosion test using a potentiostat. This electrolyte was made by mixing a specific amount of NaCl powder with distilled water to achieve a 0.1 M concentration. Figure 4 illustrates the preparation process for the materials and equipment used in this experiment.



Figure 4. Preparation of electrolyte liquid NaCl 0.1 M

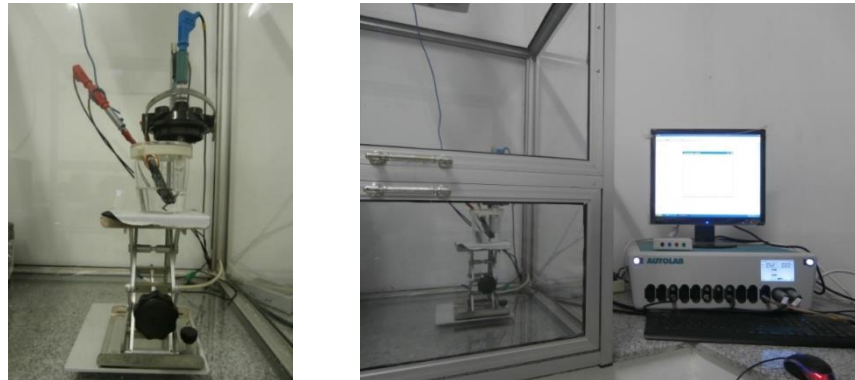


Figure 5. The cells 3 electrodes corrosion test kits with AUTOLABS tools

The three-electrode system, used with AUTOLAB tools, is a precise method for studying the corrosion behavior of materials. It consists of a working electrode (the test material), a reference electrode (with a stable and known potential, like SCE or Ag/AgCl), and a counter electrode (usually platinum or graphite) immersed in an electrolyte solution, such as 0.1 M NaCl. The AUTOLAB potentiostat/galvanostat controls the potential and measures the current between the electrodes, with NOVA software managing test parameters and data analysis. This setup allows accurate determination of corrosion potential, rates, and mechanisms through polarization curves and Tafel plots, providing valuable insights into material performance in corrosive environments. Figure 5 illustrates the configuration of the three-electrode system to perform corrosion test experiments.

## 3. Results and Discussion

### 3.1. Result

The corrosion testing process results are presented as Tafel plots generated by the NOVA software. Each variable was tested three times on each specimen to ensure result stability. Figure 6 shows the Tafel plots (example on each variation), which display the corrosion current density ( $i_{corr}$ ) in amperes based on the applied potential (V). The intersection point of the two Tafel curves provides a key value used in the Faraday equation to calculate the corrosion rate for each variation.



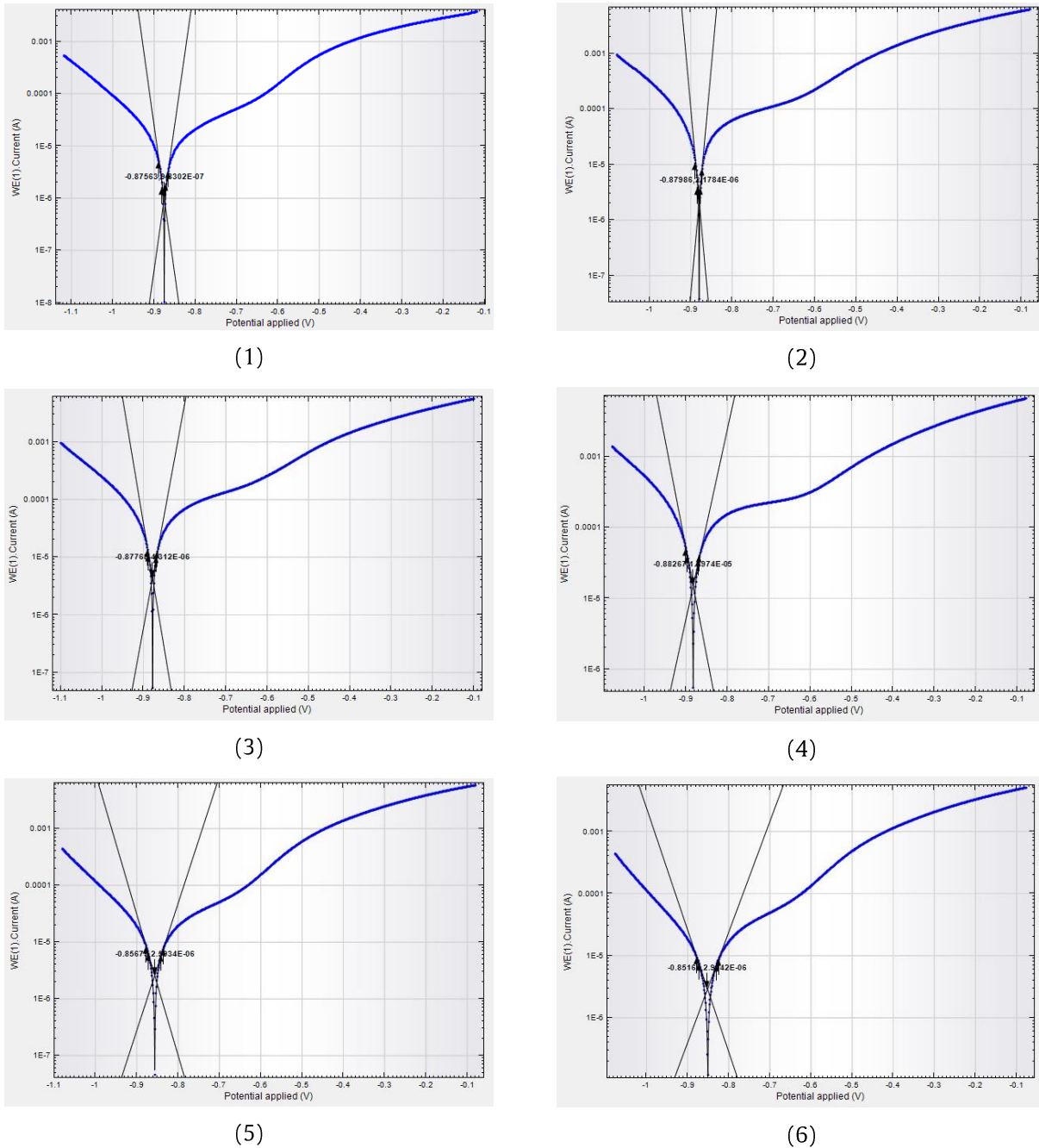


Figure 6. Graph of Tafel corrosion test results (one example on each variation).

Table 3 display the experimental results for the corrosion rates of different variations. Each variation underwent testing three times to calculate an average corrosion rate, which was then plotted to observe trends across the samples. The data reveals that the corrosion rate of the plate shows a noticeable increase to approximately 0.276 mm/year after being subjected to post-fire heat treatment at 300°C, compared to the baseline rate of 0.1 mm/year under ambient conditions. This rate escalated further to about 0.53 mm/year following heat treatment at 500°C. The corrosion rate reached its maximum at 2.527 mm/year—nearly five times higher—after heat treatment at 600°C. However, beyond this point, the corrosion rate declined to 0.37 mm/year at 700°C and experienced a slight reduction to 0.227 mm/year at 900°C.

Table 3. Results of the average corrosion rate of the experimental results.

Temperature (Celsius)	Corrosion rate (mm/year)			
	Running 1	Running 2	Running 3	Average
28	0.100	0.099	0.104	0.101
300	0.277	0.275	0.276	0.276
500	0.535	0.537	0.525	0.533
600	2.488	2.504	2.591	2.527
700	0.383	0.394	0.333	0.370
900	0.228	0.240	0.213	0.227

A comparison with the mechanical test results reported by Baihaqi et al. [9] reveals a non-linear relationship between corrosion rates and tensile strength. According to Baihaqi et al. [9], the tensile strength of post-fire mild steel plates tends to increase consistently as the temperature rises. In contrast, the corrosion rates show a different pattern: they rise sharply between 500°C and 600°C but then drop significantly between 600°C and 700°C, as illustrated in the Figure 7.

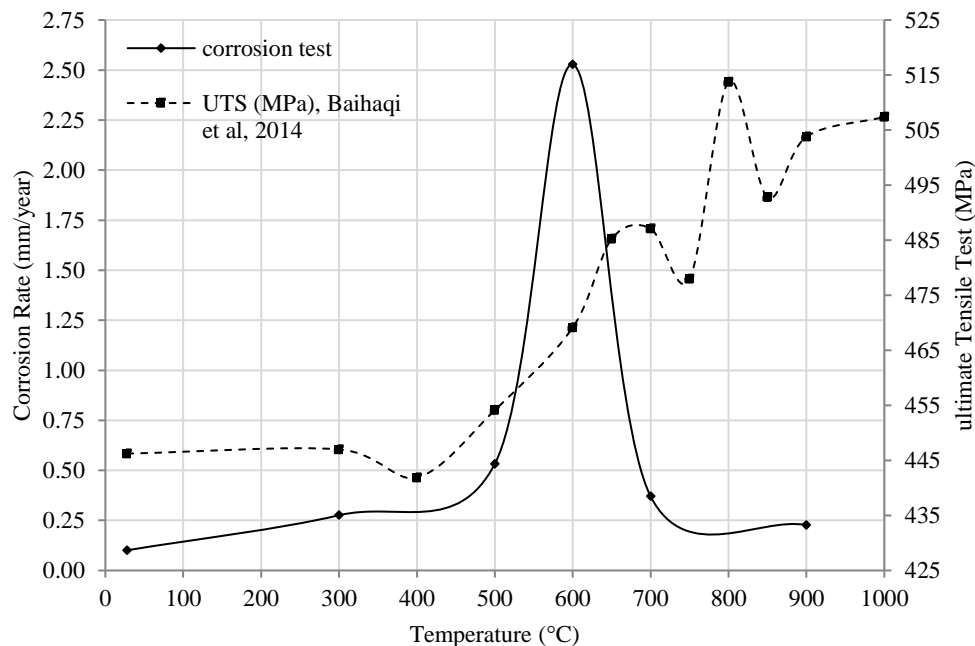


Figure 7. Corrosion rate results based on temperature vs mechanical test according to [9].

Since the burning process in this experiment uses simulation through a furnace, the real-world phenomenon of the ship hull post-fire condition cannot represent the real-world case study as presented by Komariyah et al. [10]. However, the real case study cannot present the prediction of elevated temperatures. The prediction of mechanical degradation can be shown by looking at how the steel plate and the stiffener installed in the structure change shape. The corrosion resistance in this experiment may vary with different treatments, similar to the mechanical degradation trend in this reference.

Understanding the post-fire performance of steel, particularly in marine environments, requires a combined analysis of its residual mechanical strength and corrosion behavior. Based on the literature reviewed and experimental data, a clear pattern emerges: exposure to temperatures above 600°C generally results in significant degradation of both mechanical properties and corrosion resistance, especially for mild and low-carbon steels typically used in ship structures.

From a mechanical standpoint, studies by Wang and Liu [3], Dan et al. [4], and Shi et al. [5] consistently report that yield strength, elastic modulus, and ductility begin to decline significantly when steel is exposed to temperatures exceeding 500–600°C. For instance, Dan et al. [4] found that most structural steels lose structural elasticity and begin plastic deformation above 600°C, while Wang and Liu [3] noted severe yield strength loss under both air and water-cooled scenarios at those temperatures. This degradation is further amplified in high-strength steels or when the steel undergoes prolonged exposure or rapid quenching, which may induce brittleness due to martensitic transformation.

In marine applications, corrosion behavior post-fire is equally concerning. Shen [11] and Ren et al. [12] showed that corrosion rates, even in corrosion-resistant alloys, increased drastically when exposure temperatures surpassed 700°C. This effect is primarily due to microstructural changes that create localized weaknesses, pits, or cracks, especially when fire exposure is followed by exposure to aggressive saline environments, such as seawater or splash zones. Baihaqi et al. [9] reinforced this observation, stating that although strength could increase beyond 600°C due to metallurgical changes, ductility and corrosion resistance decreased notably beyond 700°C, suggesting a limited range for safe reuse.

Komariyah et al. [10] further confirmed that annealed and softened microstructures in fire-damaged ship hulls lost resilience, especially when not subjected to protective quenching. Coupled with findings from Vukelic et al. [16], Kumar et al. [13], and Huang et al. [17], the analysis shows that corrosion pits and rust layers in splash zones lead to accelerated failure post-fire, even if mechanical strength is temporarily retained.

Therefore, to ensure safe reuse without compromising long-term integrity, both the residual strength and corrosion performance must meet minimum thresholds. The test results and literature jointly indicate that 600°C should be considered the upper threshold limit for safe reuse of mild steel in ship structures. Above this temperature, both mechanical properties and corrosion resistance degrade in a way that favors either replacement or substantial structural repair.

### 3.2. Implications for ship re-plating

Figure 7 illustrates that the corrosion rate of mild steel increases significantly between ambient temperature and 500°C. Specifically, the corrosion rate roughly doubles at 300°C and becomes five times higher at 500°C. During this temperature range, the ultimate tensile strength remains relatively stable and unchanged, indicating that mild steel is not significantly affected by heat in this range. Additionally, according to the Fe-C (Iron-Carbon) diagram, the low carbon content in mild steel prevents any noticeable changes in its microstructure at temperatures below 500°C.

At 600°C, the corrosion rate of mild steel rises sharply, becoming approximately 25 times higher than at ambient temperature. This significant increase is accompanied by a gradual rise of about 5– 8% in the ultimate tensile strength of the material. However, at 700°C, the corrosion rate drops dramatically, returning to nearly 1/25th of the rate observed at 600°C. During this temperature transition, the tensile strength continues to increase gradually but shows a slight decline at 700°C. This behavior is likely due to temperatures approaching the A1 point, where the microstructure of mild steel begins to change. As a result, the material becomes harder (a process called quenching, which involves rapid cooling), leading to an increase in tensile strength. Meanwhile, the decrease in corrosion rate can be attributed to the enhanced hardness of the steel, which makes it less susceptible to corrosion. At 1000°C, the corrosion rate of mild steel decreases slightly, accompanied by a modest increase in tensile strength. This trend suggests that the material's hardness also improves, which in turn reduces its susceptibility to corrosion and slows down the rate of material degradation. While the increase in tensile strength appears to be a positive outcome, the material's elongation decreases significantly as a result. This reduction in elongation negatively affects the material's toughness and ductility, making it more brittle and less capable of withstanding deformation [23]. In addition, after heating or firing, higher heating temperature led to increase thickness of oxidation on the steel surface because the steel surface interacts with oxygen in elevating temperature and promotes FeO, Fe<sub>2</sub>O<sub>3</sub>, or Fe<sub>3</sub>O<sub>4</sub> in certain layer thickness. After they immersed in seawater, the heated steel surface also interacts with H<sub>2</sub>O that promotes FeOH surface. Those typical passive surfaces may become barriers for the next corrosion test and may reduce corrosion rate.

The findings of this study can be applied to the process of repairing ships that have been exposed to high temperatures due to fire. If the temperature of the burned plates exceeds 600°C, it is recommended to replace them with new ones. However, if the temperature remains below 600°C, the plates can still be reused. In practice, a burning temperature of 600°C can be identified by the discoloration of the plates and by corrosion test results, which tend to show significantly higher values compared to standard corrosion rates. According to Jones [24], corrosion resistance standards, as outlined in Table 6, provide criteria for assessing the acceptability of corrosion levels.

Table 4. Comparison of corrosion resistance of materials [24].

Relative Corrosion Resistance	mpy	mm/year	μ m/year	mm/h	pm/s
Outstanding	<1	<0,02	<25	<2	<1
Excellent	1-5	0,02-0,1	25-100	2-10	1-5
Good	5-20	0,1-0,5	100-500	10-50	5-20
Fair	20-50	0,5-1	500-1000	50-150	20-50
Poor	50-200	1-5	1000-5000	150-500	50-200
Unacceptable	200+	5+	5000+	500+	200+

The guideline states that a good corrosion rate falls somewhere in the range of 0.1 to 0.5 millimeters per year. The experimental findings, on the other hand, demonstrate that the corrosion rate reaches 2.488 mm/year at 600 degrees Celsius. This rate is considered to be in the poor category according to the standard, which indicates that the condition of the material is unequivocally unacceptable. Even while the rate of corrosion decreases to less than 0.5 millimeters per year at temperatures ranging from 700 degrees Celsius to 1000 degrees Celsius, the material is still not up to the required technical standards. According to ASTM A36 [21], this is because its elongation value is lower than the minimum criterion of 23% set forth by the standard. Reusing materials that have been subjected to temperatures more than 600 degrees Celsius is therefore not suggested.

The Fe-C (Iron-Carbon) diagram provides a deeper explanation for this behavior. When the temperature of carbon steel used in ships is raised above 600°C, it approaches the temperature at which crystallization occurs, which results in a change in the crystal structure of the material. In the case of low carbon steel, which has a carbon content of approximately 0.18%, the A1 (crystallization) temperature is found to be anywhere between 700 and 750 degrees Celsius. At a temperature of 700 degrees Celsius, the experimental findings demonstrate a significant reduction in the rate of corrosion, which can be related to changes in the crystal structure of the steel. During the process of the material transitioning from its initial crystal phase, its properties, notably its resistance to corrosion, undergo several changes.

#### 4. Conclusion

This article examines how the corrosion resistance of ship-grade mild steel is affected by fire exposure at specific high temperatures. The experimental setup involved heating the steel in a furnace followed by rapid cooling with seawater to simulate real-life conditions. Laboratory tests using the 3-electrode cell method revealed that the corrosion rate of steel significantly increases at temperatures above 600°C. However, between 700°C and 1000°C, the corrosion rate decreases. This reduction in corrosion rate at higher temperatures is attributed to a significant increase in the hardness of the material after being exposed to temperatures above 600°C, which slows down the oxidation process. At 600°C, the corrosion rate peaks because the steel's crystal structure becomes unstable and undergoes changes. This instability leads to an uneven crystal arrangement, making the material more susceptible to corrosion due to weakened bonding. The article suggests that future research should focus on real-world investigations of post-fire ship hull structures and include an economic analysis to assess the feasibility of repairing fire-damaged hulls.

#### Acknowledgements

The authors sincerely thank the Chemistry Laboratory in Sepuluh Nopember Institute of Technology, Surabaya for its assistance in conducting the corrosion experiment using the three-electrode cell method.

## References

- [1] KNKT, "Data Investigasi Kecelakaan Pelayaran Tahun 2010 - 2016," Jakarta, 2016.
- [2] KNKT, "Investigation Report." Accessed: Mar. 03, 2025. [Online]. Available: <https://knkt.go.id/en/investigasi>
- [3] F. Wang and E. M. Lui, "Experimental study of the post-fire mechanical properties of Q690 high strength steel," *Journal of Constructional Steel Research*, vol. 167, p. 105966, 2020. <https://doi.org/10.1016/j.jcsr.2020.105966>
- [4] W.-J. Dan, R.-B. Gou, M. Yu, Y.-B. Ge, and T.-J. Li, "Experimental study on the post-fire mechanical behaviours of structural steels," *Journal of Constructional Steel Research*, vol. 199, p. 107629, 2022. <https://doi.org/10.1016/j.jcsr.2022.107629>
- [5] G. Shi, S. Wang, and C. Rong, "Experimental investigation into mechanical properties of Q345 steel after fire," *Journal of Constructional Steel Research*, vol. 199, p. 107582, 2022. <https://doi.org/10.1016/j.jcsr.2022.107582>
- [6] H.-T. Li and B. Young, "Post-fire mechanical properties of high strength steels," in *Proceedings of the 12th International conference on Advances in Steel-Concrete Composite Structures (ASCCS 2018)*, Universitat Politècnica de València., 2018.
- [7] X. Yan, Y. Xia, H. B. Blum, and T. Gernay, "Post-fire mechanical properties of advanced high-strength cold-formed steel alloys," *Thin-Walled Struct.*, vol. 159, p. 107293, 2021. <https://doi.org/10.1016/j.tws.2020.107293>
- [8] J. A. Gordon, S. C. Bozeman, E. C. Fischer, O. B. Isgor, and J. D. Tucker, "Heating duration effects on post-fire structural steel mechanical properties," *Fire Safety Journal*, vol. 140, p. 103848, 2023. <https://doi.org/10.1016/j.firesaf.2023.103848>
- [9] I. Baihaqi, D. Manfaat, and H. Supomo, "Karakteristik Mekanik Baja Karbon Rendah pada Konstruksi Badan Kapal Pasca Terbakar," in *Seminar Nasional Kelautan*, Surabaya: Universitas Hang Tuah Surabaya, 2014.
- [10] S. Komariyah, R. Lesmana, M. R. F. Hariadi, and S. Anggara, "Assessing post-fire material degradation: A ship structural analysis case study," in *IOP Conference Series: Earth and Environmental Science*, IOP Publishing, 2024, p. 12013.
- [11] K.-Y. Shen, "Microstructure and Properties of Super-Ferritic Stainless Steels Used for Marine Construction after Fire Exposure," *Advances in Materials Science and Engineering*, vol. 2022, no. 1, p. 6322565, 2022. <https://doi.org/10.1155/2022/6322565>
- [12] C. Ren, H. Wang, Y. Huang, and Q.-Q. Yu, "Post-fire mechanical properties of corroded grade D36 marine steel," *Construction and Building Materials*, vol. 263, p. 120120, 2020. <https://doi.org/10.1016/j.conbuildmat.2020.120120>
- [13] V. Kumar, S. K. Tiwari, and N. Sharma, "Effect of corrosion on IF-Steel in simulated-marine environment via its mechanical properties," *Materials Today Communications*, vol. 34, p. 105184, 2023. <https://doi.org/10.1016/j.mtcomm.2022.105184>
- [14] Y. Garbatov and C. Guedes Soares, "Spatial corrosion wastage modeling of steel plates exposed to marine environments," *Journal of Offshore Mechanics and Arctic Engineering*, vol. 141, no. 3, p. 31602, 2019. <https://doi.org/10.1115/1.4041991>
- [15] G. Vukelic, G. Vizin, J. Brnic, M. Brcic, and F. Sedmak, "Long-term marine environment exposure effect on butt-welded shipbuilding steel," *Journal of Marine Science and Engineering*, vol. 9, no. 5, p. 491, 2021. <https://doi.org/10.3390/jmse9050491>
- [16] G. Vukelic, G. Vizin, S. Ivosevic, and Z. Bozic, "Analysis of prolonged marine exposure on properties of AH36 steel," *Engineering Failure Analysis*, vol. 135, p. 106132, 2022. <https://doi.org/10.1016/j.engfailanal.2022.106132>
- [17] Y. Huang, X. Yu, Q. Zhang, and R. De Marco, "Corrosion performance of high strength low alloy steel AISI 4135 in the marine splash zone," *Electrochemistry*, vol. 85, no. 1, pp. 7–12, 2017. <https://doi.org/10.5796/electrochemistry.85.7>
- [18] F. Gao *et al.*, "Investigating the corrosion performance of hull steel with different microstructure in a tropical marine atmosphere," *Journal of Materials Research and Technology*, vol. 27, pp. 2600–2614, 2023. <https://doi.org/10.1016/j.jmrt.2023.10.061>
- [19] C. Zhang, R. Wang, and L. Zhu, "Mechanical properties of Q345 structural steel after artificial cooling from elevated temperatures," *Journal of Constructional Steel Research*, vol. 176, p. 106432, 2021. <https://doi.org/10.1016/j.jcsr.2020.106432>
- [20] J. Lee, M. D. Engelhardt, and E. M. Taleff, "Mechanical properties of ASTM A992 steel after fire," *Engineering Journal*, vol. 49, no. 1, pp. 33–44, 2012. <https://doi.org/10.62913/engj.v49i1.1222>
- [21] ASTM A36, "Standard Specification for Carbon Structural Steel (ASTM A-36)," West Conshohocken: United States., 2009.
- [22] ASTM G5-94, "Standard Reference Test Method for Making Potentiostatic and Potentiodynamic Anodic Polarization Measurements," 2011.
- [23] W. D. Callister Jr and D. G. Rethwisch, *Materials science and engineering: an introduction*. John wiley & sons, 2020.
- [24] D. A. Jones, *Principles and prevention*, vol. 2, no. 168. 1996.